BELLCOMM, INC.

SUBJECT: Some Considerations for Reducing the Size of Unmanned Mars Entry Probe Packages - Case 103-2

DATE: July 28, 1966

FROM: D. E. Cassidy

ABSTRACT

Parametric plots are presented to illustrate the relationship between the physical parameters of typical unmanned Mars entry probes and their influence on the guidance and terminal deceleration systems. In addition, thrust augmentation is considered as a means of reducing the size of entry probes, without affecting payload weight, and still remaining within specified guidance accuracy and decelerator deployment conditions.

FACILITY FORM 602

X66-37744 (ACCESSION NUMBER)

27 (PAGES)

CR-78822 (NASA CR OR TMX OR AD NUMBER)

X67-70705 (THRU)

2A (CODE)

30 (CATEGORY)

(NASA-CR-153014) SOME CONSIDERATIONS FOR REDUCING THE SIZE OF UNMANNED MARS ENTRY PROBE PACKAGES. CASE 103-2 (Bellcomm, Inc.) 23 p

N77-78373

Unclas

00/15 31980

INPUT BRANCH

NASA Offices and Research Centers Only

SUBJECT: Some Considerations for Reducing the Size of Unmanned Mars Entry Probe Packages - Case 103-2

DATE: July 28, 1966

FROM: D. E. Cassidy

MEMORANDUM FOR FILE

The low atmospheric pressures on Mars have led recent unmanned Mars entry studies to accept large volume, low density package designs for entry probes.[1,2] Vehicles of this type are needed to provide the low ballistic parameter (m/C_DA) necessary to aerodynamically decelerate the entry package to some acceptable descent velocity. Excess volume is undesirable, and can be more penalizing in terms of overall mission design than excess weight. This will be particularly true for an unmanned probe integrated within a manned Mars flyby spacecraft where the ancillary probe should have minimum influence on the spacecraft design.

It is desirable, then, to consider what is involved in obtaining a consolidated package of minimum size and maximum density.

Tradeoff Parameters

For a low energy Mars flyby mission during the 1975 opportunity, the entry probe will have an initial entry velocity around 30,000 fps at a 220 km altitude. This velocity is higher than was considered for the 1970-1971 opportunity unmanned probe studies[1,2] due to the higher relative velocity at Mars passage associated with the manned flyby. The Mars VM-8 model atmosphere[6], derived from the Mariner IV occultation experiments by JPL, is used for this analysis. The VM-8 atmosphere has the lowest scale height of the VM series and represents the worst case in terms of minimum entry corridor.

For an unmanned ballistic (non-lifting) entry probe, the available corridors, in terms of vacuum periapse, are presented in Figure 1. The undershoot is defined here by the maximum deployment conditions, i.e., Mach number and altitude, for a terminal aerodynamic decelerator, e.g., parachute or ballute, rather than an acceleration limit as would be the case for a manned system. The overshoot is defined by the shallowest trajectory that never leaves the atmosphere following initial entry.

Available to NASA Offices and Research Centers Only.

It is evident from Figure 1 that the corridor attainable for a given ballistic coefficient is a strong function of the maximum deployment conditions for the decelerator system, and, conversely, the ballistic parameter strongly affects the deployment conditions for a fixed corridor. This leads to tradeoffs between the guidance system, decelerator system and ballistic characteristics of the entry probe.

It is not the intention here to make these tradeoffs but to discuss what is involved in improving the packaging characteristics in terms of affecting the guidance and terminal decelerator systems constraints and by introducing possible thrust augmentation.

Packaging Tradeoffs

A vehicle configuration similar to the conceptual design of Reference 1 will be considered as typical of the type that motivated this investigation and will be referred to as the initial configuration for parameter variation pruposes:

- sphericone aerodynamic shell
- cone angle 60°
- diameter to nose radius (D/R) = 12
- diameter = 15 ft
- weight = 1850 lbs
- volume = 256 ft^3
- ballistic parameter (m/C_DA) = .2 $slugs/ft^2$

The relations between diameter, ballistic parameter, gross weight and packaging density for constant geometry are presented in Figure 2. To obtain a 30% reduction in probe diameter (D_2/D_1=.7), for example, and still maintain a constant gross weight (W_2/W_1=1), the ballistic parameter will be doubled (B_2/B_1=2) and the packaging density almost tripled ($P_2/P_1 \approx 3$). The increase in packaging density should not pose serious design constraints since the densities of these vehicles as currently conceived are particularly low.* Doubling the ballistic parameter, though, would seriously

---

*less than 4 lbs/ft^3 (Reference 2); less than 7.5 lbs/ft^3 (Reference 1).

affect the guidance and terminal decelerator systems design. This is illustrated in Figure 1 by comparing the m/C_DA of .2 to .4.

Shell Structure

The 30% reduction in diameter in the previous example will also precipitate a reduction in the structural shell mass fraction. This is of interest since the shell structural fraction is particularly large.[1,2] The structural fraction ratio is presented in Figure 3 in terms of diameter ratio and density ratio for two structural criteria. Criterion 1 was derived from Reference 5 for maximum buckling stress in a hemisphere under compressive load:

$$\text{stress} \quad \alpha \quad (\text{peak aerodynamic pressure})^{.56}$$

$$\frac{\text{shell structural weight}}{\text{vehicle weight}} \quad \alpha \quad (\text{diameter})^{.44} \quad (\text{density})^{-.56}$$

Criterion 2 represents an extreme where minimum gage thickness prevails and structural shell thickness is held constant:

$$t_s = \text{constant}$$

$$\frac{\text{shell structural weight}}{\text{vehicle weight}} \quad \alpha \quad (\text{diameter})^{-1} \quad (\text{density})^{-1}$$

It is fortuitous that at the diameter and density ratios under consideration, both structural criteria give about a 50% reduction in structural fraction. The points of intersection on Fig. 3 obviate making a choice between the two criteria but do not represent any "better" solution.

For a vehicle with an initial structural fraction of .3, this 50% reduction would correspond to a total weight reduction of 15%, while still maintaining the same internal system and payload weights. The ballistic parameter would then be held to a 1.7 growth factor, Figure 2, as compared to 2.0 where the reduced structural fraction was not considered.

It might be construed from Figure 2 that reduced structural fraction at a smaller diameter can provide some benefit in reducing the diameter without influencing the ballistic parameter. This, though, is not possible with either of the two structural criteria. For a constant ballistic coefficient, Criterion 1 states that the structural fraction varies as the square root of the vehicle weight ($Ws/_W \alpha W\ 1/2$), while from Criterion 2, the structural fraction is invariant ($Ws/_W \alpha 1$).

The structural fraction would have to vary at a faster rate than the gross weight to be effective.

The heat protection weight is assumed to be lumped into the shell structural weight even though the heat protection mass fraction does not vary the same as the structural fraction. For a constant ballistic parameter, the material fraction ablated through convective heating varies as the inverse 1/4 power of vehicle weight [3] ($\frac{W_{H.P.}}{W} \propto \frac{1}{W^{1/4}}$). The material ablated is a small fraction of the total shell, however, and should not affect the shell weight appreciably for the low m/C_DA type entry probes under consideration.

Configuration Change

So far the shell shape has been held fixed. The question of shell shape variations within the sphericone family will now be considered. The sphericone volume, ballistic parameter, surface area and length are presented in Figures 4 through 7, normalized to base diameter. For large cone angles and diameter-to-nose radius ratios, these parameters approach those of pure cones.

The effect of a sample shape variation on the packaging tradeoffs is presented in Figure 8. Here the cone angle was changed from 60° to 50° and the D/R was considered large ($\sim$ 12). A 30% reduction in diameter under these conditions results in a factor of 2.7 increase in ballistic coefficient. This new vehicle, although 30% smaller in diameter, is practically unchanged in length and volume from the initial vehicle, Figures 5 and 7. Compared to the constant configuration case, though, the length and volume are both about 45% larger; and a penalty is paid in increased ballistic parameter. The only alternative to reduce the ballistic parameter is an increase in the cone angle, which is already large.

In summary, reducing a characteristic length and maintaining the same shape will result in parameter variations according to Figure 2. The shell structural fraction variations, although not well defined, should be bracketed within the two criteria of Figure 3. Shape changes can be made following Figures 4 through 7 which alter these variations, an example of which is presented in Figure 8. Tradeoffs must then be made between the physical parameters of the vehicle, i.e., length, diameter, volume, and the guidance and terminal decelerator requirements presented in Figure 1.

Thrust Augmentation

Applying rocket thrust prior to atmospheric entry is generally less desirable than employing atmospheric drag forces to reduce the entry vehicle's velocity. This is due to the large ΔV reductions required and the relative weights involved in both schemes. On the other hand, employing rocket thrust to augment the drag braking could be desirable. Here a larger $m/C_D A$ could be employed permitting a smaller, more compact entry probe.

Two cases of thrust augmentation will be considered. Thrust will be applied either to reduce the Mach number at altitude for the terminal aerodynamic decelerator deployment or to reduce the terminal velocity to zero at the planet surface. The first case is dependent upon the maximum deployment conditions, and both cases are dependent upon the guidance accuracy.

To illustrate this situation, the velocities at 20,000 ft and 1,000 ft altitudes are presented in Figure 9 for the 30,000 fps entry velocity considered in Figure 1. The velocity at 20,000 ft is indicative of the conditions for decelerator deployment, and the velocity at 1,000 ft is conservative for the terminal velocity at surface impact.

For a typical appraisal of thrust augmentation requirements, the conditions for decelerator deployment will be M = 1.2 at 20,000 ft and a guidance accuracy corresponding to a 60 NM entry corridor. This would be "loose" guidance compared to Apollo standards, but an unmanned probe over long distances may be considerably less sophisticated. As an example, if one is to accept a $1/4^\circ$ error in flight path angle at final correction, this would correspond to about 8 NM error in corridor per Mars radius from entry. In addition, the deployment Mach number could possibly be increased;[4] but the specified conditions are similar to the recent Mars probe study[1] and will be considered conservative in terms of an attainable system.

From Figure 1 it is evident that the .2 $m/C_D A$ vehicle will satisfy the specified guidance and deployment requirements without thrust augmentation. When the vehicle diameter is reduced by 30%, as was proposed previously for the constant configuration, the ballistic parameter increases to .4 $m/C_D A$. This results in an excess velocity above M = 1.2 of about 1900 fps at 20,000 ft (M = 1.2 $\approx$ 800 fps at 20,000 ft), Figure 9. The propulsive system weight required to deliver this ΔV, assuming a .85

propellant fraction and I_{sp} = 300 sec (Figure 10), will increase the vehicle gross weight by 27%. Applying this weight increase to Figure 2, at a 2.0 factor in m/C_DA, permits only a 20% net reduction in diameter.

This approach tacitly assumed an instantaneous application of ΔV. But, this is not possible in a real case. Therefore, the distance, normalized to the thrust-to-initial weight ratio, required to achieve a terminal velocity in a vacuum is presented in Figure 11. This distance is slant range and must be multiplied by the sine of the flight path angle to convert to differential altitude. To reduce 1900 fps to M = 1.2 at 20,000 ft, as in this example, requires about 12,000 ft of slant range for a T/W_i of 4. Since the average flight path angle is about -15°, the corresponding altitude differential would be 3100 ft. The average velocity across this 3100 ft altitude for the no propulsion case, Figure 12, is about 3100 fps compared to about 2100 fps when thrust is applied. Neglecting gravity, since the acceleration of gravity is an order of magnitude less than drag, the change in velocity due to drag with altitude is:

$$\frac{dV}{dH} \approx \left[\frac{\rho}{2\ m/C_DA\ \sin\gamma} \right] \bar{V} \quad .$$

The terms in the brackets can be taken as average values across the altitude interval and then assumed to have the same average value for the thrust and no-thrust case. Thus, the change in velocity due to drag (drag ΔV) for small altitude changes is proportional to the average velocity across the interval, i.e., $\frac{\Delta V}{\Delta H} \propto \bar{V}$. Since the average velocity in the thrust augmented case will be 68% of the no-thrust case, the drag ΔV will be 32% less. This will result in an increased propulsive ΔV to 2200 fps instead of the 1900 fps for the instantaneous ΔV case and a propulsive system weight increase to 32% of the probe weight, Figure 11. Applying this increased weight to Figure 2 results in about a 1% to 2% increase in the diameter compared to the instantaneous ΔV case. Although the penalty in this example is small, larger m/C_DA and steeper entry angles will be more costly. As would be expected, increasing the T/W_i will bring the finite and instantaneous thrust cases together; but decreasing the T/W_i will have the opposite effect.

To summarize the first application of thrust augmentation, two points are to be considered. The increased propulsive

system weight will tend to negate the gain in diameter reduction, and, secondly, low propulsive thrust-to-weight will require larger ΔV due to reduced drag ΔV.

Terminal Propulsive Braking

The case where the propulsive system is used to provide terminal landing capability is now considered. At 1000 ft altitude, Figure 9, the .4 m/C_DA vehicle has a velocity of about 830 fps. As in the previous case, the ballistic parameter has been doubled following the 30% reduction in diameter. The propulsive system weight required to deliver this 830 fps ΔV is about 11%, Figure 10. Since the propulsive system is acting as a terminal landing device, the aerodynamic decelerator would not be a required on board system. This loss in weight would probably just balance the propulsive system weight. Even so, an additional 11% of probe weight would still permit a 26% diameter reduction. If one is to consider the difference in finite and instantaneous ΔV, the slant range presented in Figure 14 at a $T/W_i = 4$ results in a small increase in propulsive system fraction and a negligible increase in diameter ratio. Generally, the loss in drag ΔV at the lower velocities closer to the ground would be small.

The time for this propulsive maneuver is presented in Figure 14 normalized to T/W_i. Thus, for a $T/W_i = 4$, the propulsive time would be something over 5 seconds.

In summary, the terminal propulsive braking scheme takes full advantage of drag ΔV, and only a small penalty is paid for the reduced drag ΔV over the interval of thrust application. The diameter reduction is greater than the previous case, but sequence timing becomes critical. In addition, reduced weight at the smaller diameter will be realized without the requirement for an aerodynamic decelerator.

Conclusion

The diameter of an entry probe can be reduced but at the expense of increasing the requirements on the guidance system and/or terminal retardation system or by reducing the gross weight. Gross weight reductions can accompany diameter reduction due to improved structural fraction. This effect cannot be used, though, to reduce the diameter at a constant ballistic parameter. Thrust can be used to augment drag braking either to provide more favorable conditions for terminal decelerator system deployment or to

act as a terminal landing system. The former case will provide reductions in diameter but not to the extent obtainable in the latter case.

D. E. Cassidy

1021-DEC-jld

Attachments
References, Figures

Copy to
Messrs.

P. E. Culbertson - NASA/MTL
J. H. Disher - NASA/MLD
F. P. Dixon - NASA/MTY
E. Z. Gray - NASA/MT
T. A. Keegan - NASA/MA-2
D. R. Lord - NASA/MTX
M. J. Raffensperger - NASA/MTE
L. Reiffel - NASA/MA-6
A. D. Schnyer - NASA/MTV
W. B. Taylor - NASA/MLA

M. A. Silveira - MSC/ET-25
W. E. Stoney - MSC/ET
J. M. West - MSC/AD

R. C. Harris - MSFC/R-AS-VP
B. G. Noblitt - MSFC/R-AERO-XA
F. L. Williams - MSFC/R-AS-DIR

J. P. Claybourne - KSC/EDV-4
R. C. Hock - KSC/PPR-2
N. P. Salvail - KSC/MC

F. G. Allen
G. M. Anderson
C. L. Davis
E. L. Gruman
D. R. Hagner
P. L. Havenstein
J. J. Hibbert
J. A. Hornbeck
B. T. Howard
D. B. James
H. S. London
J. Z. Menard
I. D. Nehama
G. T. Orrok
I. M. Ross
R. L. Selden
R. V. Sperry
T. H. Thompson
W. B. Thompson
J. M. Tschirgi
R. L. Wagner
Central Files
Department 1023
Library

REFERENCES

1. Mars Probe Entry From Orbit, AFCO/RAD Contract No. NAS 1-522A, January, 1966.

2. Advanced Voyager/Beagle for Saturn V, GE-RSD No. 70036, March, 1964.

3. "Approximate Heating Calculations for Mars Atmospheric Entry," Bellcomm Memorandum for File, D. E. Cassidy, January, 1966.

4. Feasibility of Parachute Operation at High Mach Numbers and Dynamic Pressures, R. Turner, J. C. McMullen, presented at AIAA, Third Aerospace Science Meeting, New York, January, 1966.

5. Effects of Mars Atmospheric Uncertainties on Entry Vehicle Design, J. M. Spiegel, Aerospace Engineering, December, 1962.

6. Atmosphere Data to Alter Voyager Design, Aviation Week & Space Technology P.P. 66-69, Nov. 22, 1965.

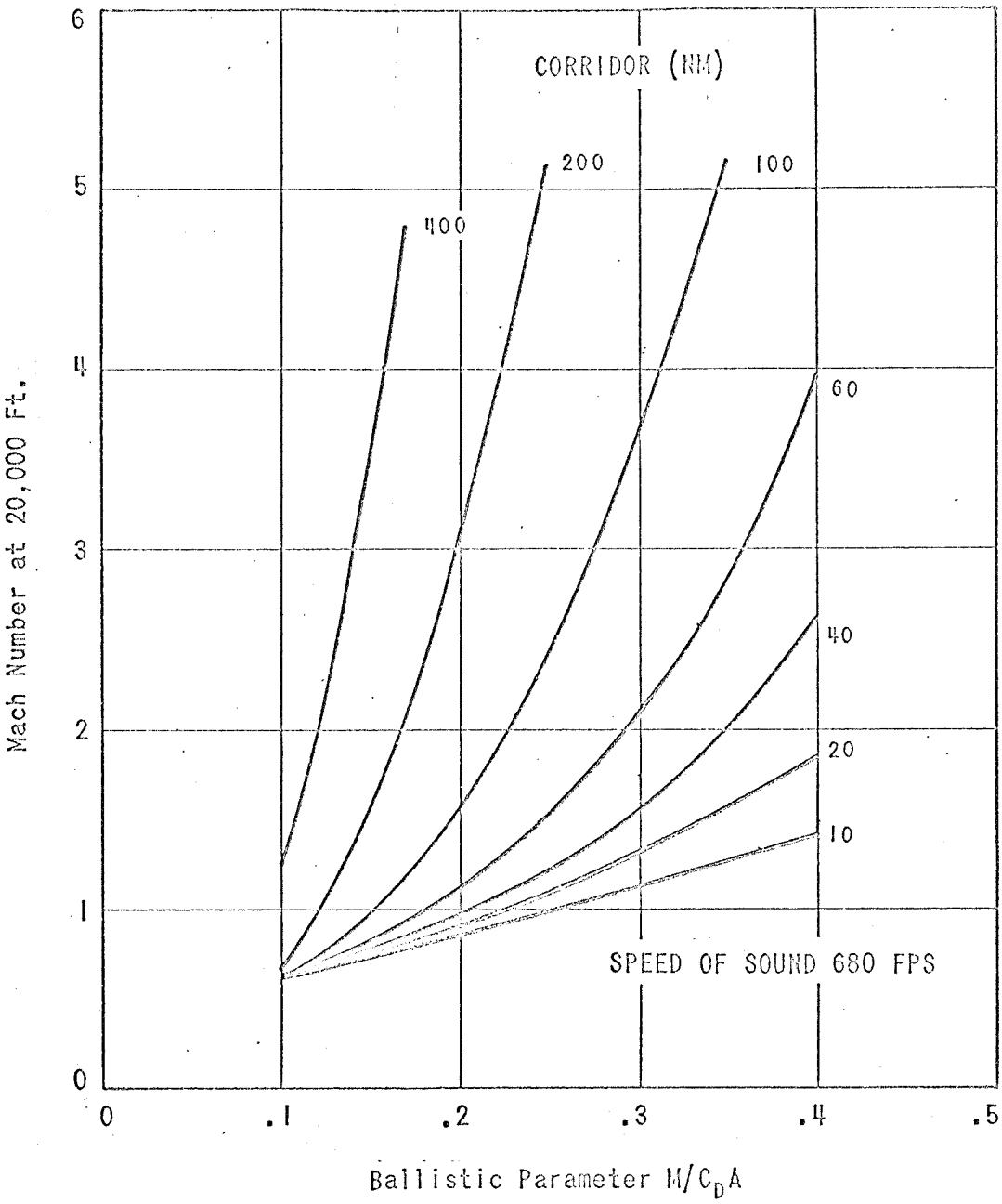

FIGURE 1 - MARS VM-8 ATMOSPHERE
V = 30,000 FPS/220 KM

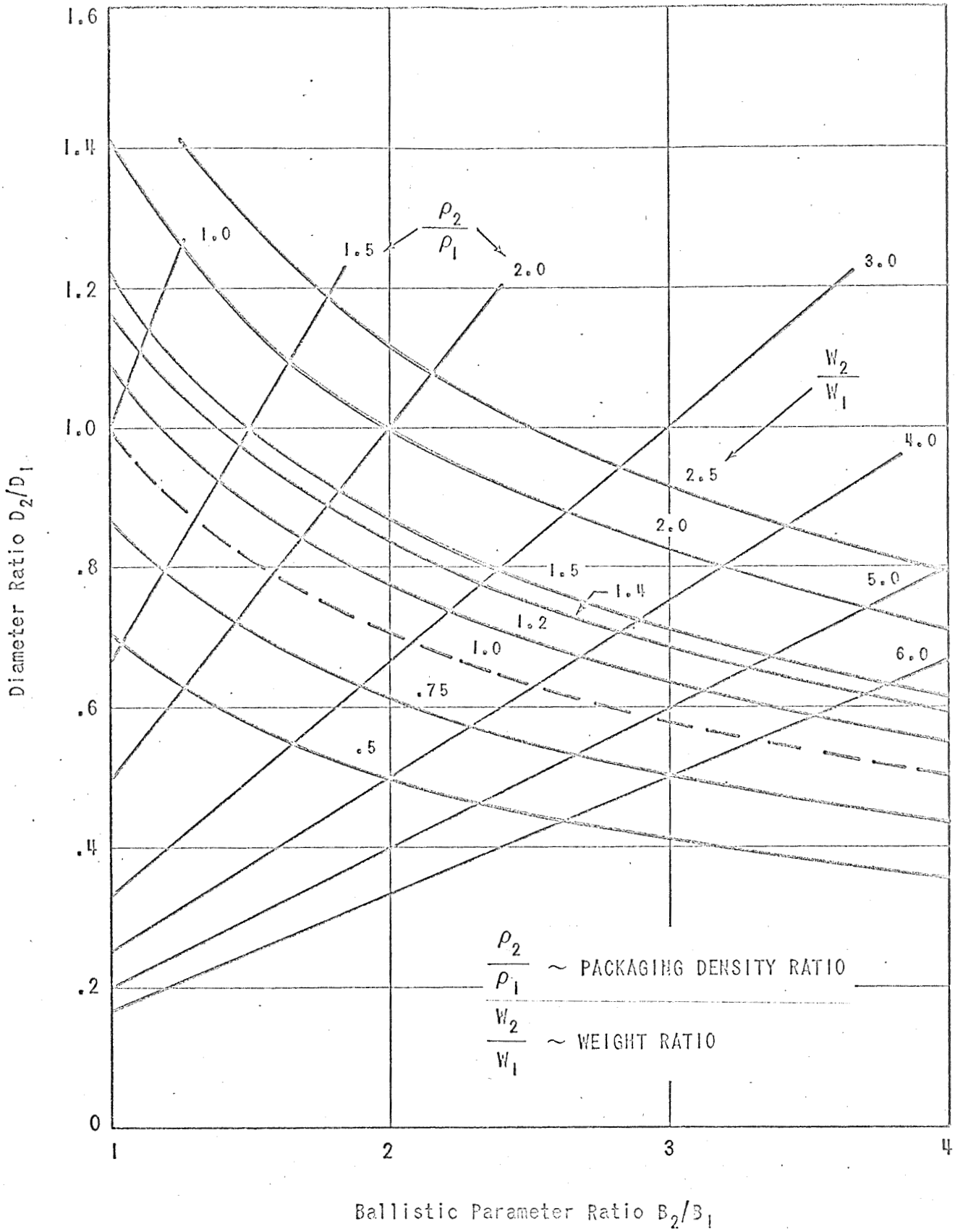

FIGURE 2 - PACKAGING REQUIREMENTS FOR CONSTANT GEOMETRIC SHAPE

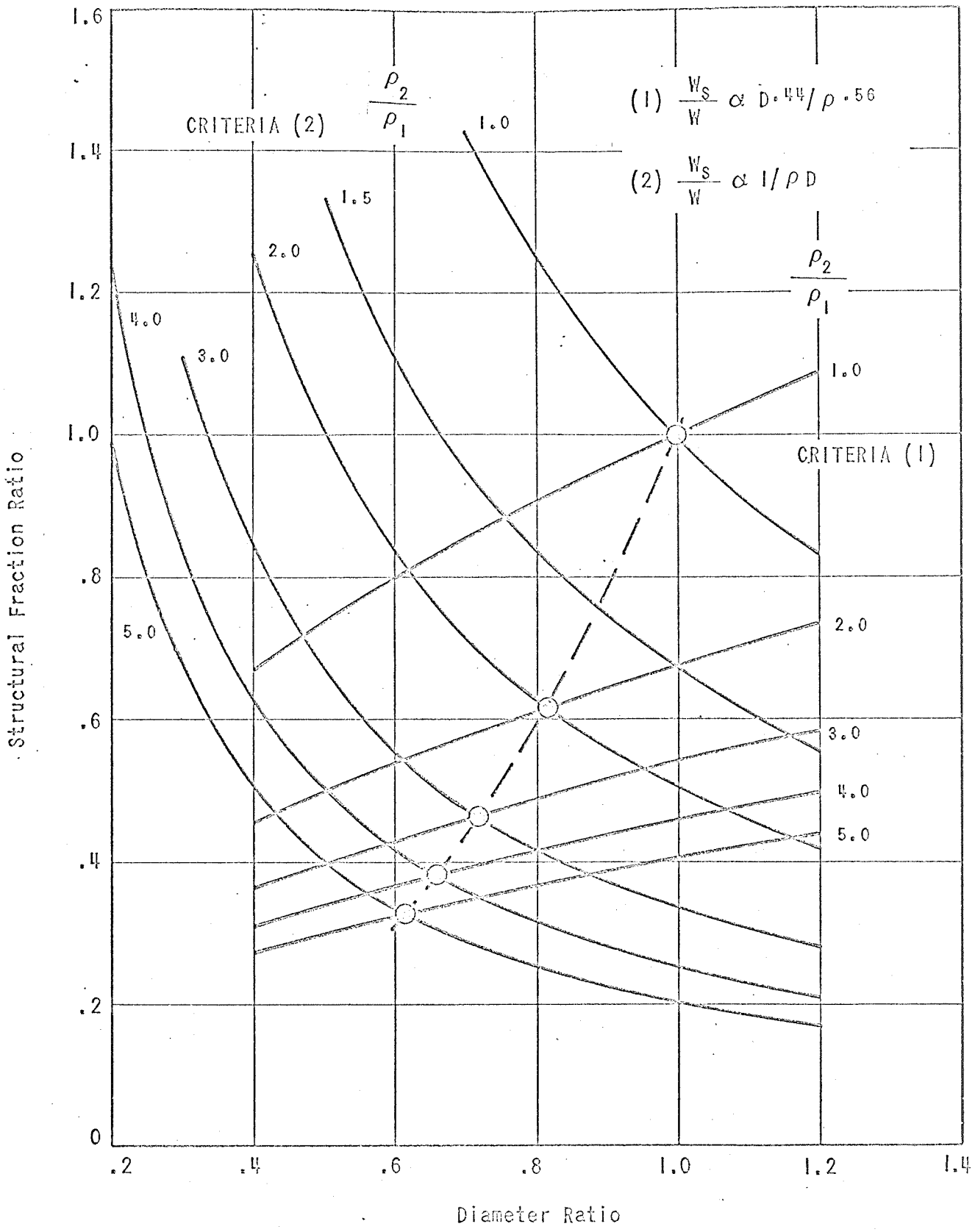

FIGURE 3 - STRUCTURAL FRACTION

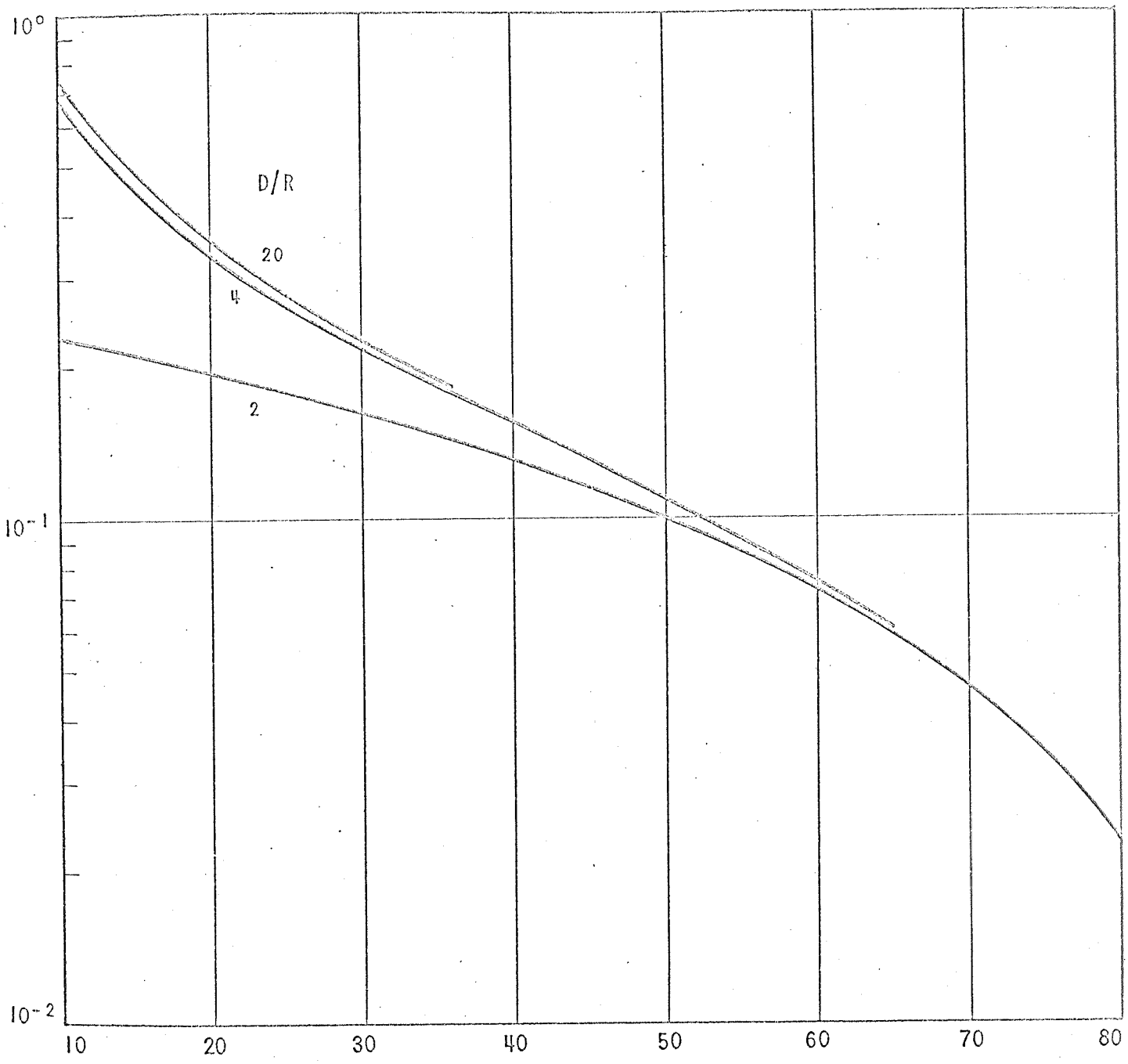

FIGURE 4 - VOLUME NORMALIZED TO DIAMETER

$$\frac{V}{D^3}$$

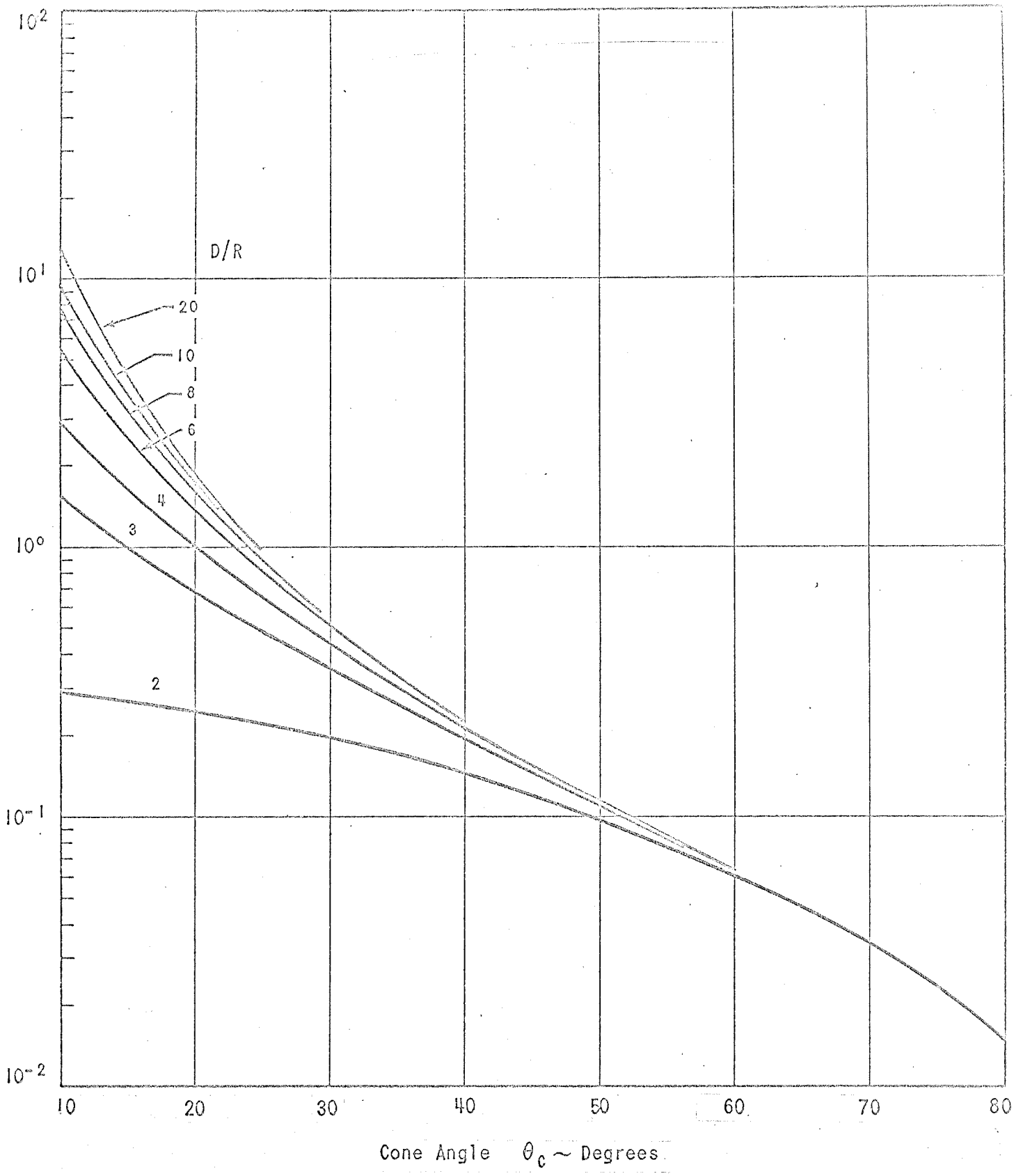

FIGURE 5 - BALLISTIC PARAMETER NORMALIZED TO BASE DIAMETER AND PACKAGING DENSITY

$$\frac{I}{\rho . D} \qquad \frac{W}{C_D A}$$

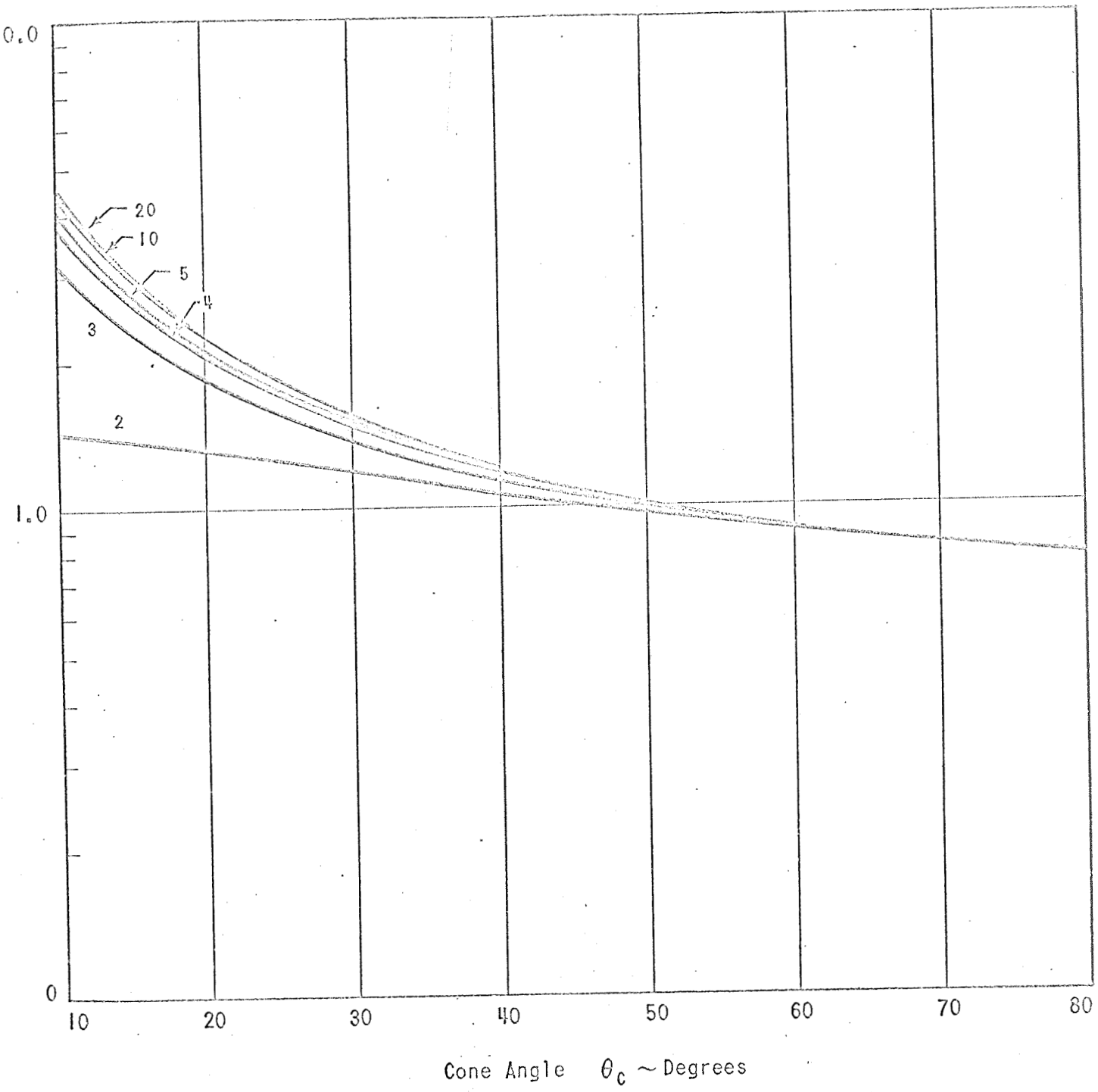

FIGURE 6 - SURFACE AREA (LESS BASE AREA) NORMALIZED TO BASE DIAMETER

$$\frac{S}{D^2}$$

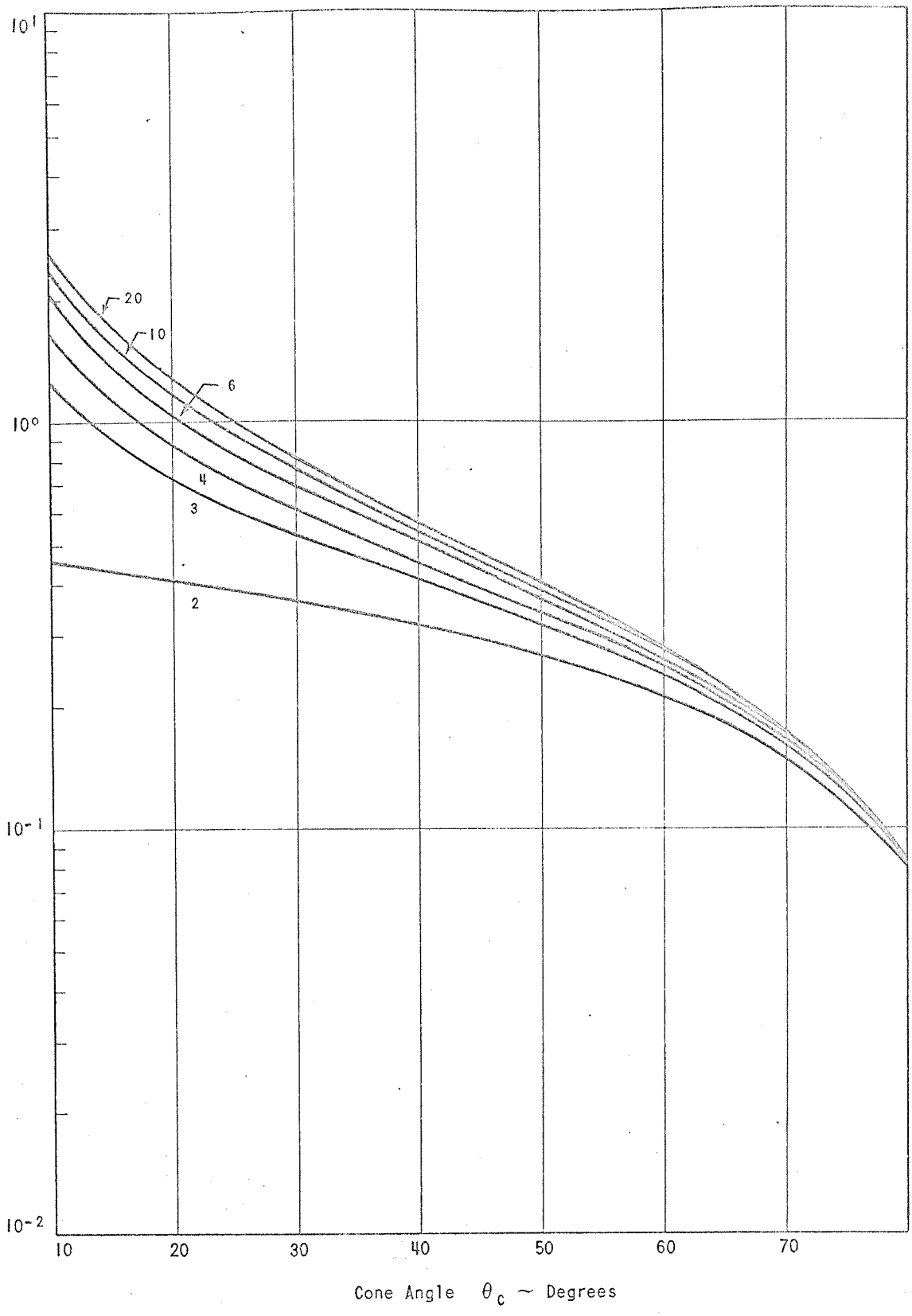

FIGURE 7 - LENGTH NORMALIZED TO BASE DIAMETER

$\frac{L}{D}$

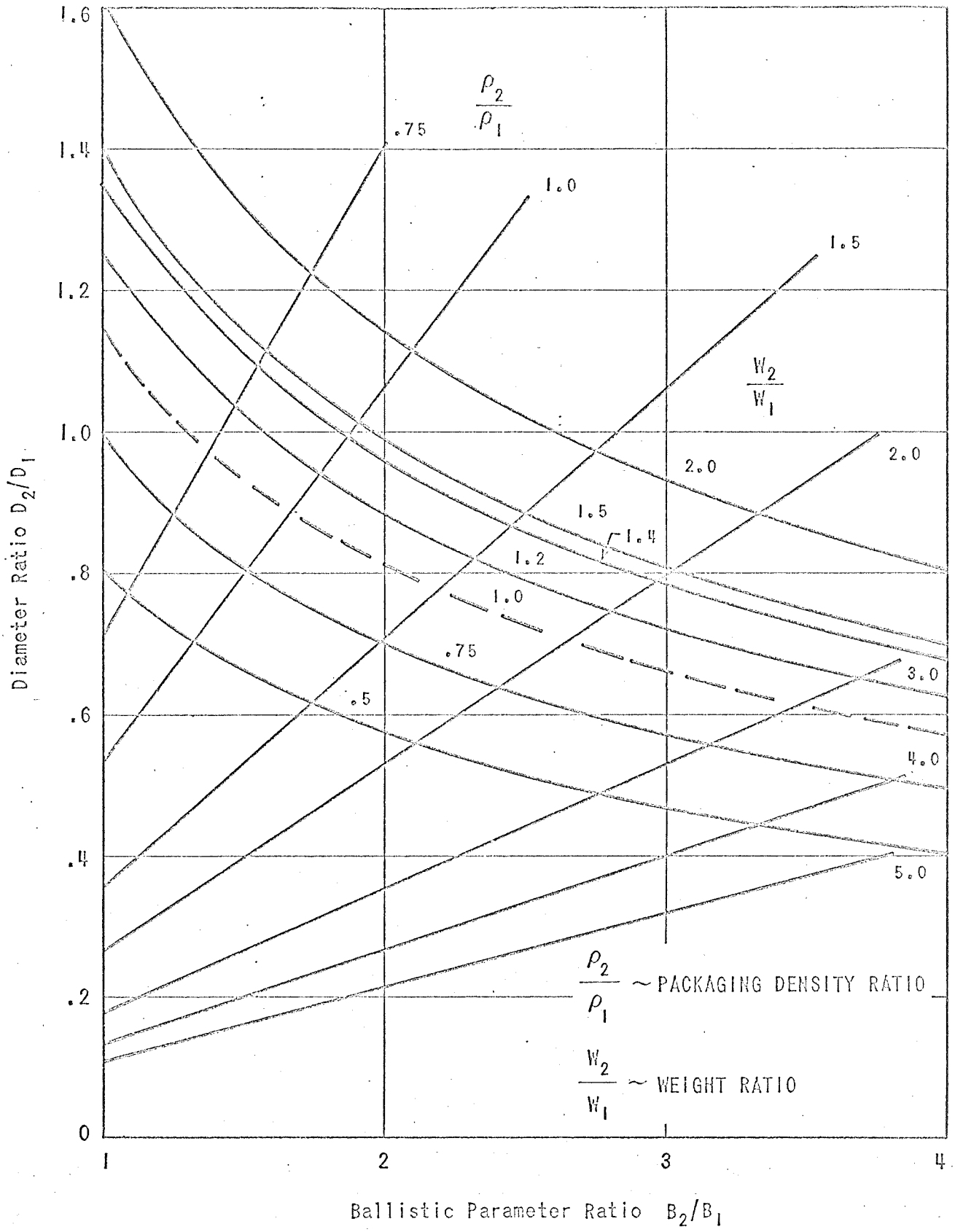

FIGURE 8 - PACKAGING REQUIREMENTS GOING FROM θ_c = 60° TO 50°

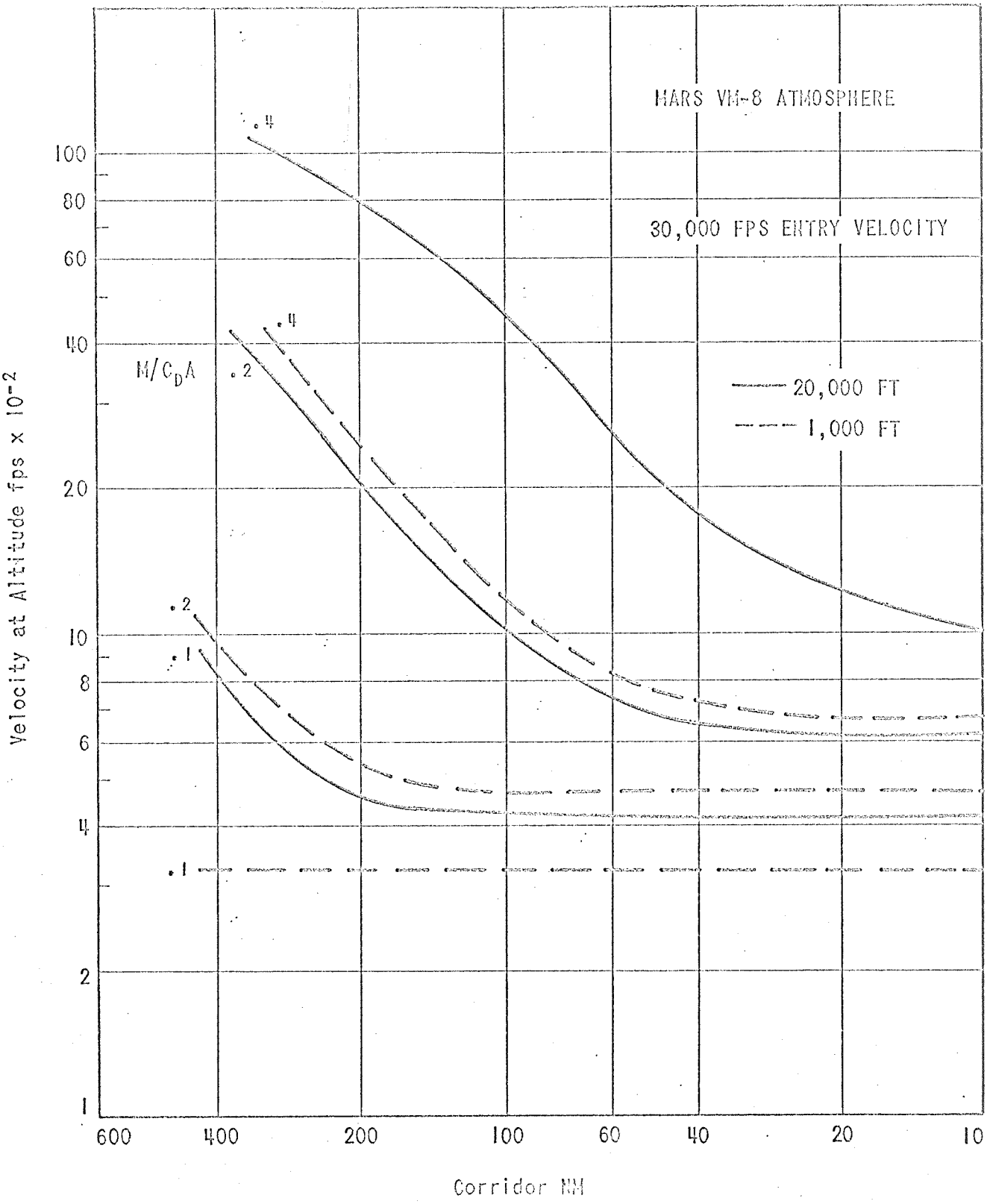

FIGURE 9 - VELOCITY AT ALTITUDE FOLLOWING BALLISTIC ENTRY

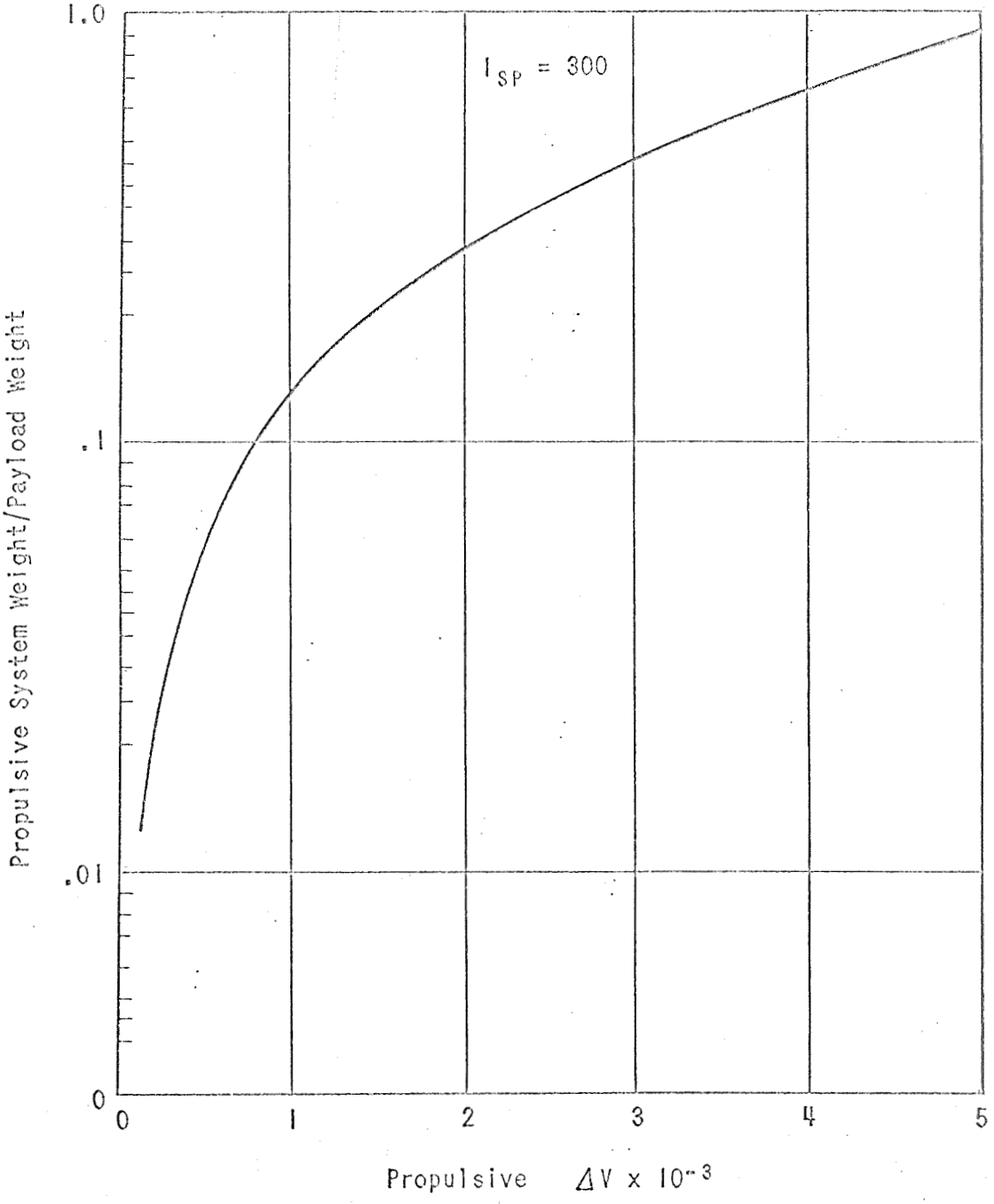

FIGURE 10 - PROPULSIVE SYSTEM WEIGHT

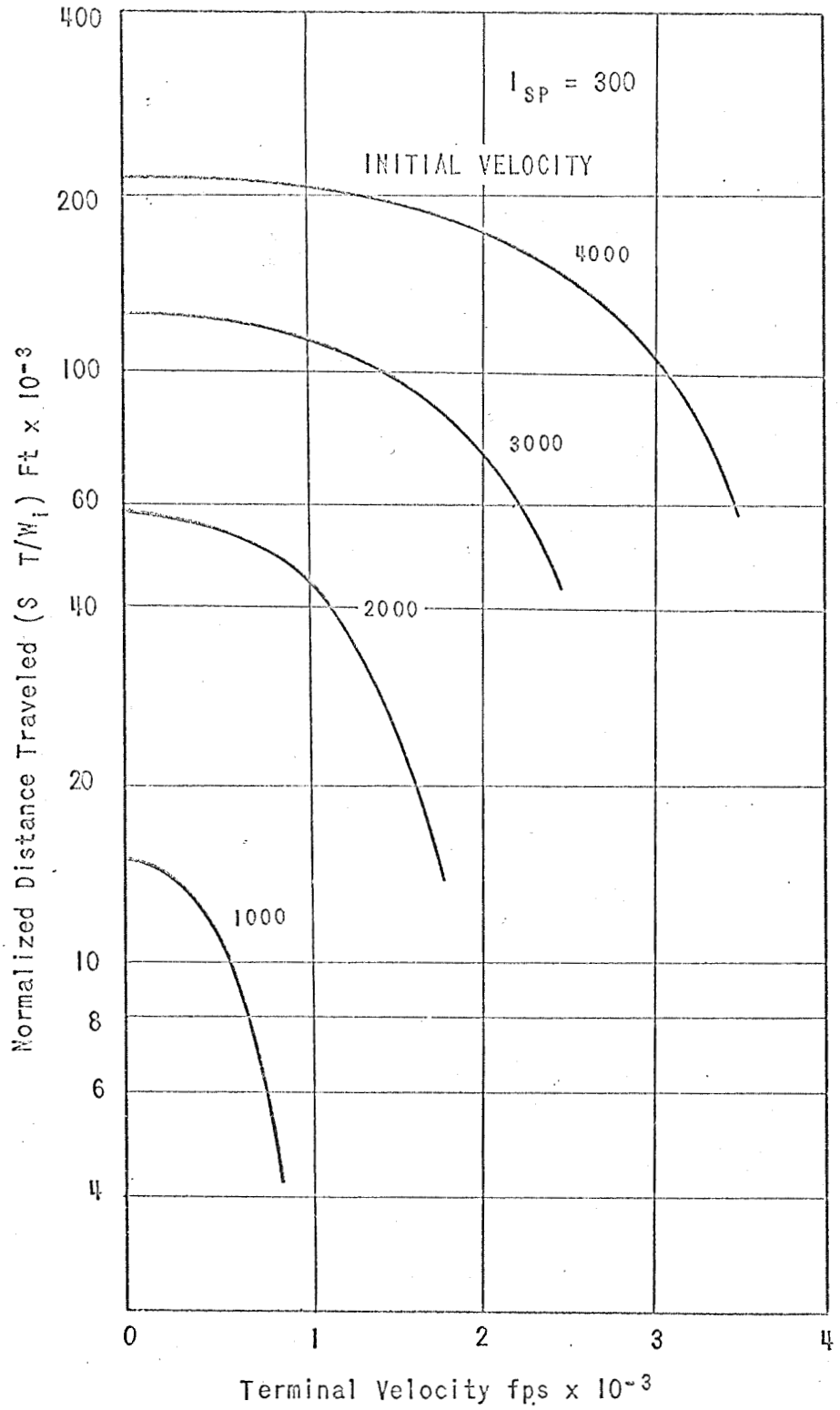

FIGURE II - DISTANCE REQUIRED FOR VELOCITY REDUCTION WITH ROCKET PROPULSION

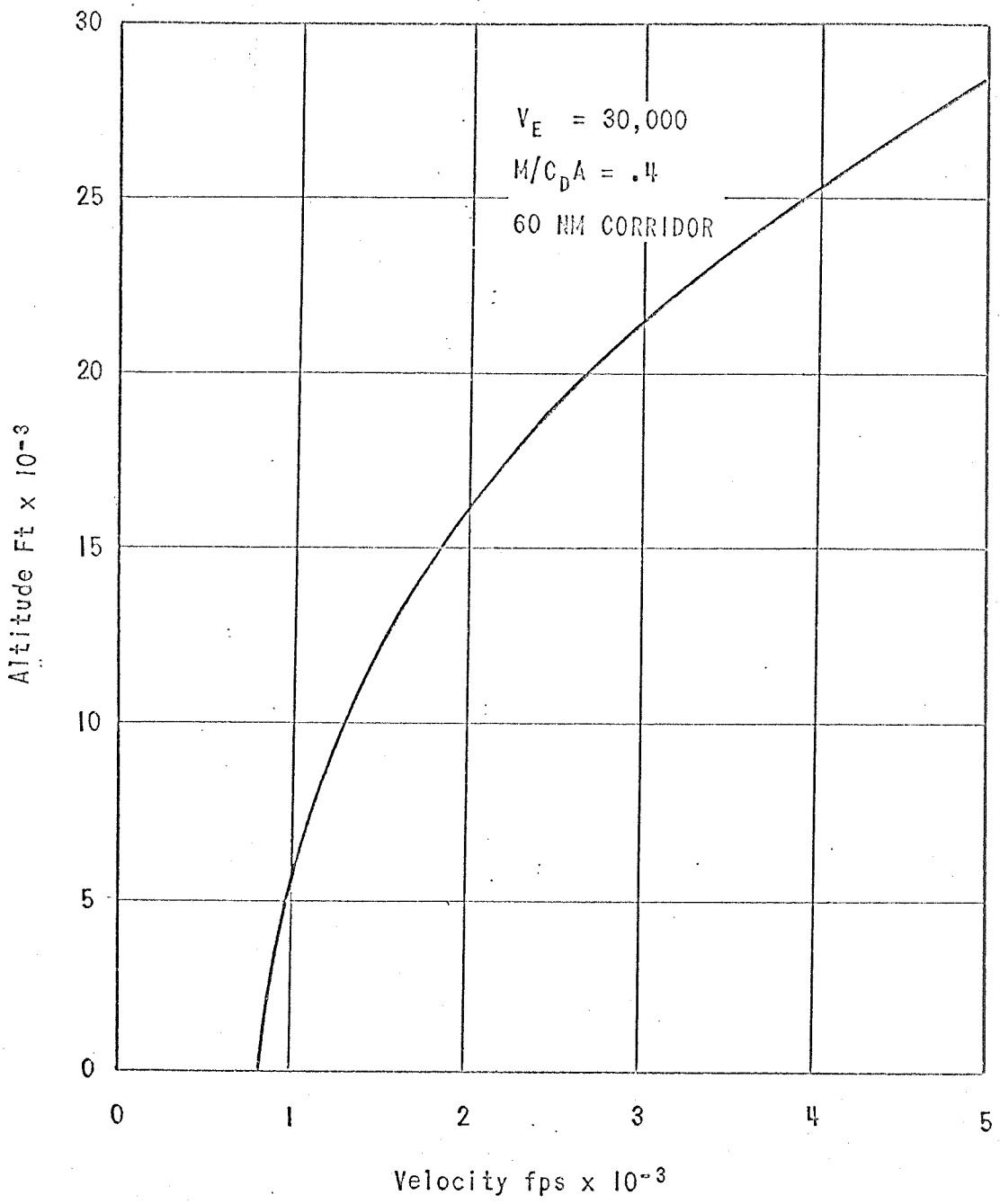

FIGURE 12 - ALTITUDE - VELOCITY

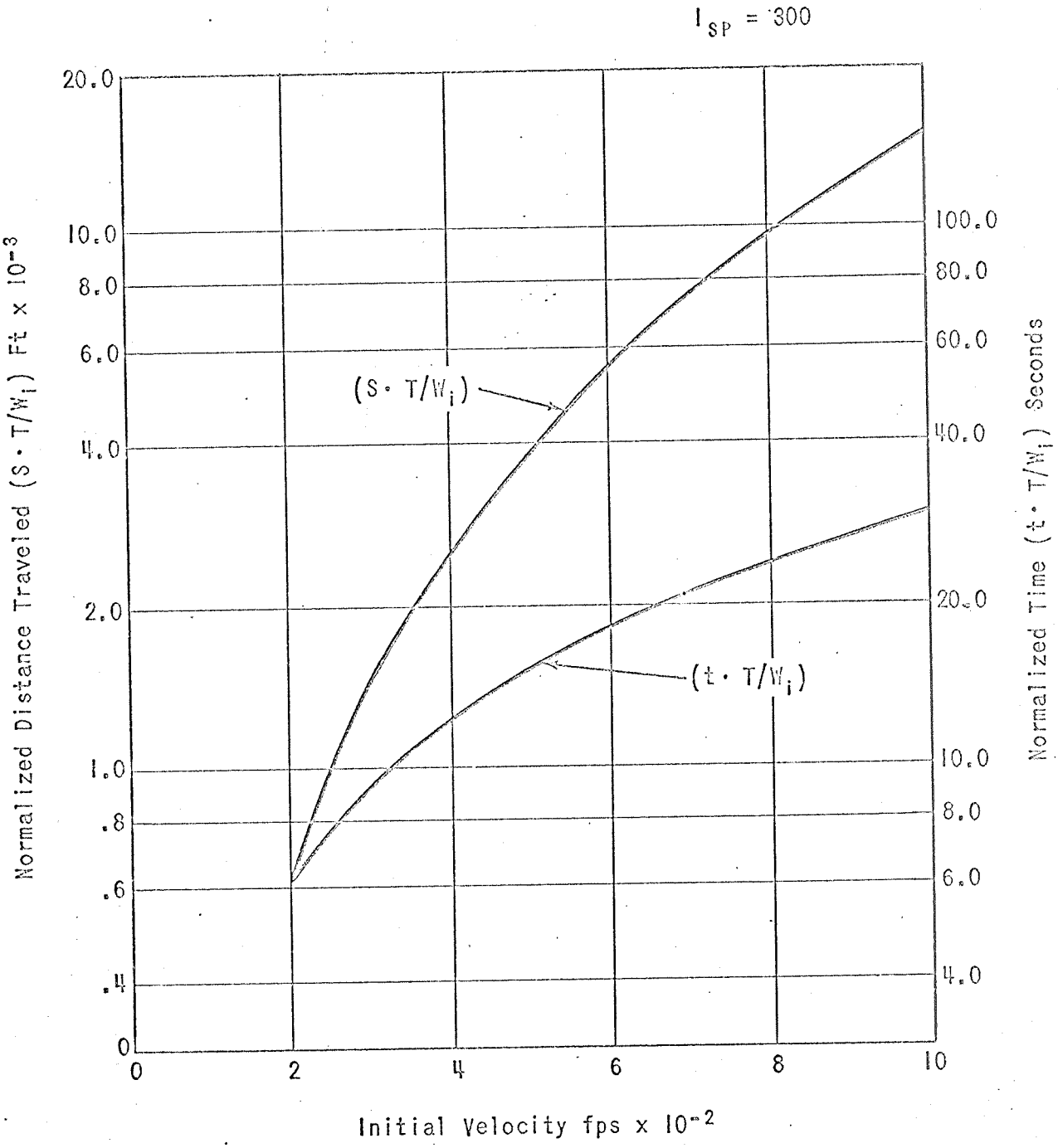

FIGURE 13 - DISTANCE AND TIME REQUIRED TO REDUCE VELOCITY TO ZERO